Journal of Enhanced Heat Transfer, 26(4):345–363 (2019)

EXPERIMENTAL STUDY OF THE THERMOHYDRAULIC PERFORMANCE OF WATER/ETHYLENE GLYCOL–BASED GRAPHITE NANOCOOLANT IN VEHICLE RADIATORS

A.R. Akash,[1] Arvind Pattamatta,[1,] & Sarit K. Das[2]*

[1]*Department of Mechanical Engineering, Indian Institute of Technology Madras, Chennai–600036, India*

[2]*Department of Mechanical Engineering, Indian Institute of Technology Ropar, Rupnagar Punjab–140001, India*

*Address all correspondence to: Arvind Pattamatta, Department of Mechanical Engineering, Indian Institute of Technology Madras, Chennai–600036, India; Tel.: +91-44-2257-4654, E-mail: arvindp@iitm.ac.in

Original Manuscript Submitted: 9/2/2018; Final Draft Received: 12/10/2018

Water/ethylene glycol (W/EG) mixture is a common heat transfer fluid in vehicle radiators that exhibits poor thermal performance. It can be substituted by nanocoolants (nanofluids as coolant) to enhance the overall heat transfer performance of radiators. However, addition of nanoparticles to enhance heat transport may be accompanied by a simultaneous increase in pumping power. In the present study, an experimental evaluation of thermohydraulic performance of graphite nanocoolant (W/EG-based graphite nanofluid as coolant) in vehicle radiators is carried out by utilizing an in-house test rig. The thermal performance of the nanocoolant and the base fluid is compared at the same Reynolds numbers, coolant mass flow rates, and pumping power. The overall heat transfer coefficient is augmented with the use of a nanocoolant, while comparing with the same Reynolds number and coolant flow rate criteria. The enhancement is higher at lower air and coolant mass flow rates and gradually decreases as the flow rates increases. The same pumping power comparisons demonstrate that for low pumping power cases the overall heat transfer coefficient of the nanocoolant is higher than the base fluid, and the trend converses as the pumping power increases to higher values. The performance index, which indicates the net enhancement or diminution of thermal performance relative to the pumping power, is relatively more for graphite nanocoolant at lower coolant and air mass flow rates but diminishes in experiments with higher flow rates. This study shows that an analysis for finding the sweet spot is essential before applying graphite nanocoolant in vehicle radiators.

KEY WORDS: *heat transfer enhancement, nanofluids, automotive radiator, performance index, pumping power*

1. INTRODUCTION

A radiator is an air-cooled cross-flow heat exchanger used in vehicles to remove excess heat generated in engines. It has a vital impact on a vehicle's weight and on the design of the

NOMENCLATURE

A	total area of heat transfer, m^2
$A_{cs,rt}$	cross-sectional area of radiator tube, m^2
$A_{s,rt}$	surface area of radiator tube, m^2
$C_{p,c}$	specific heat of coolant, J/kgK
D	circular tube diameter, m
$D_{h,rt}$	hydraulic diameter of radiator tube, m
F	LMTD correction factor
f	friction factor
h	local heat transfer coefficient, W/m^2K
L	length of radiator tube, m
LMTD	logarithmic mean temperature difference
$\dot{m}_a$	air mass flow rate, kg/h
$\dot{m}_c$	coolant mass flow rate, kg/h
n	total number of radiator tubes
P	temperature effectiveness
ΔP	pressure drop across radiator, Pa
ΔP_{bf}	pressure drop across radiator for base fluid, Pa
ΔP_{nc}	pressure drop across radiator for nanocoolant, Pa
Q	total heat transfer, W
R	heat capacity rate ratio
Re	Reynolds number
TEM	transmission electron microscope
$T_{a,in}$	air inlet temperature, K
$T_{a,out}$	air outlet temperature, K
$T_{c,in}$	coolant inlet temperature, K
$T_{c,out}$	coolant outlet temperature, K
T_w	radiator tube wall temperature, K
U	overall heat transfer coefficient, W/m^2K
U_{bf}	overall heat transfer coefficient for base fluid, W/m^2K
U_{nc}	overall heat transfer coefficient for nanocoolant, W/m^2K
V_c	velocity of coolant, m/s
x	distance along streamwise direction, m

Greek Symbols

ϕ	volume fraction
ε	effectiveness
μ	dynamic viscosity of fluid, Pa.s
σ	uncertainity
ρ_{bf}	density of base fluid, kg/m^3
ρ_c	density of coolant, kg/m^3
ρ_{np}	density of nanoparticle, kg/m^3

Subscripts

a	air
bf	base fluid
c	coolant
cs	cross-sectional
in	inlet
nc	nanocoolant
np	nanoparticle
out	outlet
s	surface
w	wall

front-end module, which in turn has a strong influence on the vehicle's aerodynamic behavior. For decades, many studies have been conducted to enhance the heat transfer capability of radiators by employing several techniques such as different fin types and materials, various tube inserts or vortex generators, and roughened or perforated surfaces (Bergles and Manglik, 2013). Most of the techniques concentrate on the optimization in the configurational and geometrical viewpoint and are nearly saturated in their role of heat transfer enhancement.

Enhancing the properties of working fluid is an alternate technique to upsurge the heat transfer. Research has been conducted by suspending milli- to micrometer-sized particles in working fluids to enhance its heat transfer by intensifying the thermal conductivity (Ahuja, 1975; Liu et

al., 1988) but the application was limited because of its abrasive nature, clogging, higher pressure drop, and sedimentation. After a series of experiments at Argonne National Laboratory, the concept of dispersing higher conductivity nanometer-sized particles in working fluid instead of bigger particles was introduced and became popular as "nanofluids." Choi and Eastman (1995) showed theoretically that one of the potential benefits of nanofluids is the dramatic reduction in heat exchanger pumping power. The phenomenal heat transport capability of nanofluids has attracted the attention of many researchers around the world, and its application expands to several areas including laser cooling and smart cooling of automotive and electronic components. Thermal conductivity and viscosity are the most crucial thermophysical parameters influencing the heat transport capability of working fluids. In literature, a phenomenal enhancement in thermal conductivity has been reported in proportion with an increase in the particle concentration and bulk temperature of the nanofluids (Xuan and Li, 2000; Eastman et al., 2001; Das et al., 2003). The viscosity of nanofluid is influenced by numerous parameters such as volume fraction, temperature, pH, size, shearing rate, and shape (Meyer et al., 2016). Even though nanofluids have higher viscosity, slurries up to 20% volume fraction incurred a small additional pressure drop than single-phase fluids at similar flow rates (Liu et al., 1988).

Forced convective heat transfer studies can be used to inspect the practical applicability of nanofluids. The internal forced convective heat transfer of various nanofluids has been reported by several researchers, and most of the studies were carried out with metal oxide nanofluids such as γ-Al_2O_3 (Pak and Cho, 1998; Wen and Ding, 2004; Vajjha et al., 2010; Utomo et al., 2014; Bianco et al., 2018; Sandhu et al., 2018), TiO_2 (Pak and Cho, 1998; Vajjha et al., 2010; Azmi et al., 2016), ZrO_2, SiO_2, and CuO (Heris et al., 2006; Liao et al., 2010; Vajjha et al., 2010). Relatively higher augmentation in heat transfer compared to corresponding base fluids were reported in each of these studies. The metallic [copper (Li et al., 2003)] and nonmetallic [multiwalled carbon nanotube (Utomo et al., 2014; Walvekar et al., 2016), graphene (Akhavan-Zanjani et al., 2016), and graphite (Yang et al., 2005)] nanoparticle-based dispersions have confirmed higher heat transfer at low volume fractions.

Heat transfer research shows that nanofluids can be used to enhance heat transfer in several types of heat exchangers. The possibility of substituting nanofluids in cross-flow heat exchangers (radiators) instead of convectional coolants for cooling of engines was also reported. In a theoretical study, Leong et al. (2010) evaluated a 3.8% improvement in overall heat transfer coefficient and an 18.7% reduction in the frontal area of the radiator with a coolant containing 2% copper nanoparticles. Lv et al. (2010) adopted a numerical method to analyze the cooling of an internal combustion engine using nanofluids, and a remarkable enhancement in heat transfer with a tolerable increase in pumping power was reported. The average heat transfer coefficient of a radiator is experimentally analyzed in numerous studies and remarkable augmentation in the performance with various nanofluids such as Al_2O_3 (Peyghambarzadeh et al., 2011; Nieh et al., 2014), TiO_2 (Nieh et al., 2014; Hussein et al., 2014), CuO (Peyghambarzadeh et al., 2013), SiO_2 (Hussein et al., 2014), multiwalled carbon nanotube (Teng and Yu, 2013; Chougule and Sahu, 2014; M'hamed et al., 2016), and graphene (Selvam et al., 2017) was reported. In their study, Peyghambarzadeh et al. (2011, 2013) used the ε-NTU method to calculate the overall heat transfer coefficient in a radiator and reported similar maximum 9% enhancement for CuO and Fe_2O_3 nanofluids compared to water. They also reported that a decrease in nanofluid inlet temperature, increase in air/nanofluid velocity, and nanoparticle concentration caused an enhancement in the overall heat transfer coefficient. Nieh et al. (2014) had reported that TiO_2 nanocoolant showed higher heat transfer performance than Al_2O_3 nanocoolant with maximums of 25.6%, 27.2%, 6.1%, and 2.5% of enhanced ratios of heat dissipation capacity, efficiency

factor, pressure drop, and pumping power, respectively. Teng and Yu (2013) had used three different concentrations (0.1, 0.2, and 0.4 wt%) of multiwalled carbon nanotube nanofluids and reported that the nanofluid with lower concentration (0.1 wt%) shows supreme improvement of 14.1% and 12.8% in efficiency factor and heat exchange capacity, respectively, with a 4.9% increase in pumping power compared to ethylene glycol/water base fluid.

The previous studies conclude that the application of nanocoolants enhances the performance of radiators. Nevertheless, many existing heat transfer studies on radiators evaluate only the coolant side heat-transfer coefficient, whereas in a cross-flow heat exchanger, assessment of the overall heat transfer coefficient (U) is essential because it represents the net output and is dependent on both the air and coolant side heat-transfer coefficients. Another important concern while using nanofluid as a coolant in radiators is about the additional pumping power required for the same heat transfer to occur, which has a direct impact on the energy utilization efficacy. Oliet et al. (2007) estimated the additional pumping power because the pressure drop across the radiator is in the range of 0.1 to 6 W for a conventional coolant (W/EG mixture) flow-rate range of 500–2500 kg/h. Although similar statistics about the extra pumping power are required in the case of the inclusion of nanoparticles, statistics proportionate with the heat transfer enhancement are rare in literature. The majority of the experimental heat transfer studies on single tubes as well as radiators used metal-oxide nanofluids. The nonmetallic (e.g., graphite, graphene, etc.) nanofluids have prominent heat transfer properties over oxide nanofluids. Still, experimental studies using nonmetallic nanocoolants are rare in literature. Graphite is one of the most abundant and inexpensive minerals, showing excellent thermophysical properties, and to the best knowledge of the authors, heat transfer studies using graphite nanofluid in radiators is not available in the literature.

In Teng and Yu (2013), it was reported that the addition of more nanoparticles to increase the heat transfer of nanocoolant has an adverse effect in terms of higher pumping power. So in the present study, a dilute nanocoolant (0.1 wt%) is chosen to understand the flow dynamics and thermal performance. Present work involves the preparation and characterization of studies such as conductivity, viscosity, zeta potential, transmission electron microscope (TEM), and experimental studies on the radiator setup with W/EG and graphite nanocoolant. The overall heat transfer coefficient (U) calculated using the logarithmic mean temperature difference (LMTD) method is used to evaluate the thermal performance of the nanocoolant compared to the base fluid for a given/fixed coolant mass flow rate, Reynolds number, and pumping power. The influence of various parameters such as coolant Reynolds number, coolant and air mass flow rates on the pumping power, and coolant side and overall heat transfer coefficient in an industrial vehicle radiator (Mahindra Maximo) are also studied.

2. PREPARATION AND CHARACTERIZATION OF NANOCOOLANT

Graphite nanoparticle is characterized by TEM and a zeta analyzer. Figure 1(a) represents the TEM image of the nanoparticle. The average size of the nanoparticle flake is observed to be 4 μm. For the synthesis of the graphite nanocoolant, the base fluid is prepared initially by mixing deionized water with ethylene glycol in equal ratio (50:50). Then the base fluid is agitated with sodium dodecyl sulfate (SDS) at its critical micelle concentration (8.2 mMol/L). After, the amount of graphite nanoparticle required to prepare the coolant with a weight percentage of 0.1 is dispersed bit by bit in this mixture by means of a mechanical stirrer for 45 min. Afterward, the sonication is done by utilizing a probe type ultrasonicator (Q500, QSonica, USA) for 1 h, which provides a uniformly mixed homogeneous nanosuspension with good stability.

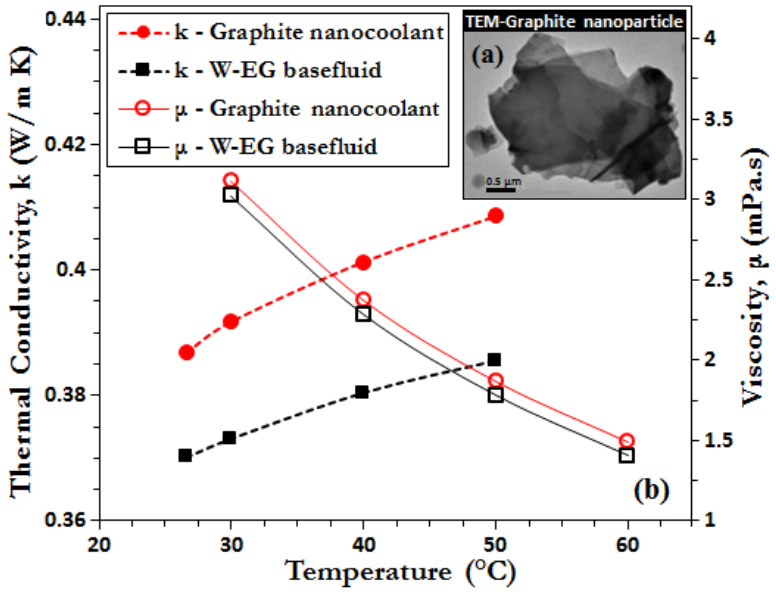

FIG. 1: (a) TEM image of graphite nanoparticle, (b) variation of thermal conductivity and viscosity as a function of temperature

Zeta potential, or ζ potential, is an abbreviation for electrokinetic potential in colloidal systems, and its absolute value is one of multiple indications of stability of dispersion. Dispersions with high absolute zeta potential value are electrically stabilized, and zeta potential values (positive or negative) larger than 30 mV are adequate to confirm the stability of dispersion in liquids of low ionic strength (Lee et al., 2008). The pH of the medium is the most significant factor that influences zeta potential. Huang et al. (2009) studied the effect of pH on the stability behavior of water-based Al_2O_3 and copper nanofluids by measuring the absorbency and zeta potential and reported that within the pH range of 7.5–8.9 these dispersions show a large value of zeta potential and good stability. The isoelectric point (IEP) is the pH at which a certain particle is electrically neutral in the statistical mean or carries no net electrical charge. To attain larger zeta potential, the pH of dispersion must be considerably away from the IEP (Berg et al., 2009). The IEP of graphite is reported to be less than 3.3 (Zuccaro et al., 2015). Dispersions with a highly alkaline nature—for example, a pH value more than 10—are not suitable for practical applications (Suganthi and Rajan, 2012).

The pH of the prepared graphite nanofluid is measured using a pH digital meter (Make: Deep Vision). Before measurements, the instrument is calibrated using buffer solutions of pH 7 and 4. The nanofluid is observed to be at pH 8.04, and the value is away from the IEP (pH 3.3) and noticeably less than the higher alkaline pH value. For measurement of zeta potential, 0.1 wt% concentration of graphite nanofluid was not useful. Instead, a dilute (0.05 wt%) graphite nanosuspension was used. The apparent zeta potential value measured by the Malvern ZS analyzer (Malvern Instruments Inc., London, UK) is –40.3 mV, where the negative charge shows the influence of anionic dispersant SDS. It is sufficiently higher than the threshold value (± 30 mV), which indicates an adequate stability of the engineered nanocolloid used in the current study.

2.1 Thermophysical Property Evaluation

Thermal conductivity of graphite nanocoolant is measured using the TCi-Thermal Conductivity Analyzer over a range of 30°C to 50°C as given in Fig. 1(b). It is observed that the graphite nanocoolant exhibits enhancement in thermal conductivity compared to the base fluid. The thermal conductivity of W/EG base fluid increases from 0.368 to 0.382 as the temperature increases from 30°C to 50°C. The thermal conductivity augmentation of the nanocoolant (0.385 to 0.45 W/mK) with temperature is 13% more than that of base fluid. Das et al. (2003) reported the stochastic motion of nanoparticles influenced by the temperature and heat flow inside the base fluid as the major reason for the remarkable enhancement of nanocoolant thermal conductivity. Higher thermal conductivity of the nanocoolants at elevated temperatures supports smart cooling effects at higher temperatures.

The dynamic viscosity of graphite nanocoolant and the W/EG base fluid is measured at a range of temperatures with an automated microviscometer (Anton Paar-AMVn) and is also plotted in Fig. 1(b). The presence of graphite nanoparticles increases the viscosity of the base fluid. However, the concentration of graphite nanocoolant used in the present study is small, hence the influence of particle loading has a much lesser effect. Because of this, the pressure drop that is a direct function of fluid viscosity can be almost equal to that of the base fluid. Hence we can expect that the graphite nanocoolant for small concentration will incur little penalty in pumping power as compared with W/EG base fluid of comparable flow rates. With an increase in temperature the base fluid viscosity also decreases asymptotically, and both coolants show a similar trend. The same kind of viscosity reduction with increasing temperature for base fluid and nanofluid was reported by Pak and Cho (1998).

3. EXPERIMENTAL SETUP AND PROCEDURE

Figure 2 represents a schematic of the experimental setup used in the current study. A photographic view of the test section, which is an industrial automobile radiator manufactured by Mahindra for their truck model Maximo, is illustrated in Fig. 3. The experimental setup comprises a tank attached with a proportional–integral–derivative controlled alternating current heater to store the coolants (either the base fluid or graphite nanocoolant) at a specified temperature. From the tank the coolant is pumped to the inner tubes in a tube heat exchanger by using a centrifugal pump (Crompton mini master self-priming) at a required flow rate, for a controlled temperature rise. The coolant mass flow rate can be controlled by regulating the main and bypass valves. A constant temperature water circulatory system (JULABOCORIO CD-300F refrigerated/heating circulator) is used to circulate hot water through the outer tube of the heat exchanger. Using this arrangement, a controlled thermal load in the system is achieved and the coolant temperature at the exit of the tube can be maintained. The exit of the heat exchanger is then fed to a micromotion coriolis mass flow meter (EMERSON-CMF025), which constantly measures the mass flow rate ($\dot{m}_c$) and density (ρ_c) of the fluid. The coolant from the mass flow meter then flows to the inlet of the radiator, and the outlet is connected to the tank to complete the loop. A differential pressure transmitter (YOKOGAWA, EJA110E-JHS4J-912EB) is used to measure the pressure drop across the radiator.

The coolant is not pressurized, and all the experiments are conducted with atmospheric pressure in the experimental loop. A fan with a shroud is bolted onto the radiator to draw air over the radiator tubes to cool the hot coolant flowing inside the radiator. The air mass flow rate is controlled by varying the input voltage and current of the fan through a variable direct current

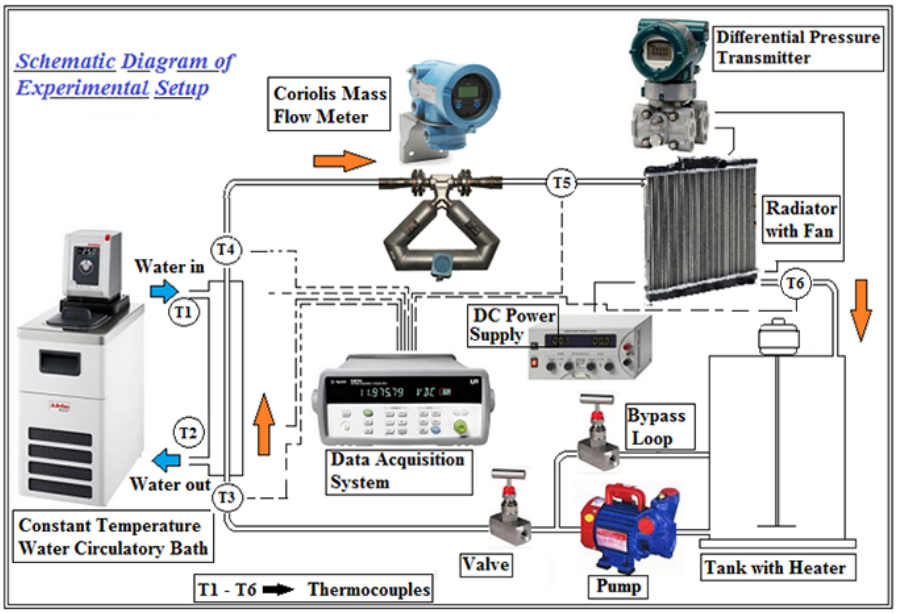

FIG. 2: Schematic diagram of the experimental setup

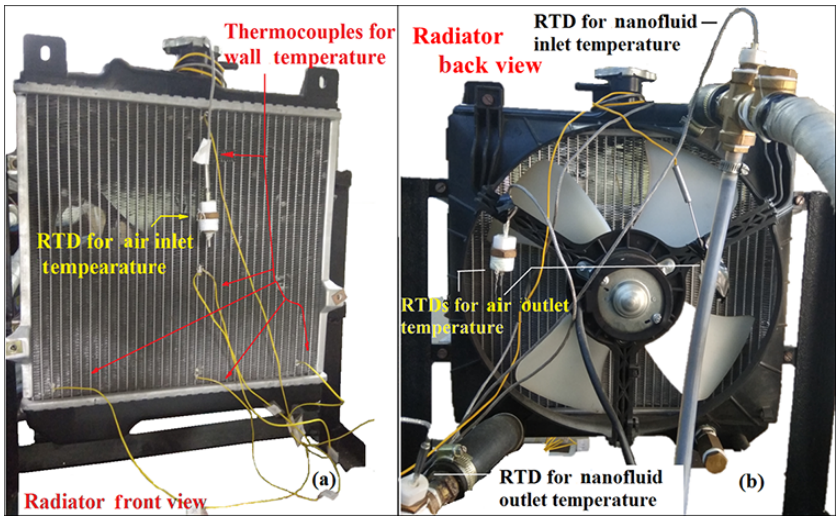

FIG. 3: Radiator (a) front view, (b) back view

power supply (Elektro Automatik, EA-PS 3016-40B). A probe-type hot wire anemometer (Testo 445) is used to measure the air velocity at various exit locations of the fan shroud. The dimensions of the vehicle radiator used for the current study is given in Table 1. The temperature at different locations of the radiators is measured using resistance temperature detectors (RTDs) and thermocouples, and their positions are shown in the photographs of the radiator's front and back views [Figs. 3(a) and 3(b)]. An RTD is used to measure the air inlet temperature ($T_{a,in}$)

TABLE 1: Radiator dimensions

Radiator height	305 mm
Radiator breadth	19 mm
Radiator width	335 mm
Number of tubes	33
Tube length	305 mm
Tube breadth	17 mm
Tube width	2 mm
Tube wall thickness	0.15 mm
Average fin pitch	1.575 mm
Fin width	7.5 mm
Fin length	19 mm
Fin thickness	0.15–0.2 mm

and thermocouples that are attached to the outer side of tube, which are used to measure the wall temperature at six different points as shown in Fig. 3(a). The maximum temperature drop across the tube thickness in all cases is measured to be less than 0.01°C due to the small thickness and the high conductivity of the aluminum tube wall. This temperature drop is negligibly small compared to the thermocouple uncertainty itself; therefore, the temperature measured at the tube outer wall is used in calculations. The coolant (W/EG base fluid and graphite nanocoolant) inlet and outlet temperatures ($T_{c,in}$, $T_{c,out}$) and the air outlet temperature $(T_{a,out})$ are measured at several positions using RTDs as illustrated in Fig. 3(b). The air inlet temperature is measured using an RTD 25 mm away from the radiator to avoid any influence from the hot coolant flowing inside the radiator. Another two RTDs are kept at the radiator outlet, immediately after the exit of the fan shroud, to measure air outlet temperature. The RTDs and thermocouples are connected to a data acquisition system (Keysight Technologies, 34970A) to monitor the experiments and to gather useful measurement data. The density of air corresponds to the fan shroud exit temperature; the average air velocity and the fan shroud exit area are used to calculate air mass flow rate in each case.

4. DATA REDUCTION AND CALCULATION OF HEAT TRANSFER

The maldistribution in radiator tubes is neglected with the assumption of equal coolant supply in all flat tubes, and the Reynolds number through each tube is calculated using Eq. (1).

$$\text{Re} = \frac{\dot{m}_c * D_{h,rt}}{n * \mu * A_{cs,rt}} \quad n = \text{number of parallel tubes in the radiator} \tag{1}$$

The experimental data collected by the data acquisition system is used to calculate the coolant side heat transfer, overall heat transfer, and required pumping power. The overall heat transfer coefficient (U) of the radiator is calculated using the LMTD method, as shown in Eq. (2).

$$Q = \dot{m}_c C_{p,c}(T_{c,in} - T_{c,out}) = UAFLMTD \tag{2}$$

The logarithmic mean temperature correction factor (F) is calculated graphically using the method given in Shah and Sekulic (2003) using the parameters for temperature effectiveness (P) and heat capacity rate ratio (R) as shown in Eq. (3).

$$P = \frac{T_{a,out} - T_{a,in}}{T_{c,in} - T_{a,in}}, \quad R = \frac{T_{c,in} - T_{c,out}}{T_{a,out} - T_{a,in}} \tag{3}$$

LMTD for the cross-flow heat exchanger is calculated using Eq. (4).

$$LMTD = \frac{(T_{c,in} - T_{a,out}) - (T_{c,out} - T_{a,in})}{ln\frac{(T_{c,in} - T_{a,out})}{(T_{c,out} - T_{a,in})}} \tag{4}$$

The correlation based on the idea of the liquid-particle mixture theory proposed by Pak and Cho (1998) is used to calculate the specific heat of the nanofluid.

$$C_{p,nc} = \phi * C_{p,np} + (1 - \phi) * C_{p,bf} \tag{5}$$

where $C_{p,nc}$, $C_{p,np}$, $C_{p,bf}$ are the specific heat of the nanocoolant, nanoparticle, and base fluid, respectively, and ϕ is the volumetric concentration of the nanoparticle in the nanocoolant.

The percentage of augmentation in the overall heat transfer coefficient while using a nanocoolant instead of the base fluid is calculated as shown in Eq. (6).

$$\%\ \text{Enhancement in UA} = \frac{[(UA)_{nc} - (UA)_{bf}] * 100}{(UA)_{bf}} \tag{6}$$

Equation (7) is used to calculate the average heat transfer coefficient of the radiator tube. Three K-type thermocouples are used to measure the wall temperature at three different locations of a single radiator tube, and the average wall temperature (T_w) is calculated. The difference between the averaged coolant and wall temperature values in the radiator is used as the temperature potential for heat transfer coefficient.

$$h = \frac{\dot{m}_c C_{p,c}(T_{c,in} - T_{c,out})}{A_{s,rt} * n * \left(\frac{(T_{c,in} + T_{c,out})}{2} - T_w\right)} \tag{7}$$

The pressure drop in the vehicle radiator is measured using a differential pressure transmitter and is used to calculate the friction factor for nanocoolant and base fluid as shown in Eq. (8).

$$f = \frac{2 * \Delta P * D_{h,rt}}{\rho_c * n * L * V_c^2} \tag{8}$$

Pumping power is a significant parameter that must be expressed together with the overall heat transfer coefficient in the thermohydraulic performance analysis of the radiator. Equation (9) is used to calculate the pumping power using the experimentally measured pressure drop across radiator, mass flow rate, and density of coolant. Hence the pumping power calculated in the present study is for flow across the radiator alone and not for the whole loop.

$$\text{Pumping power} = \frac{\dot{m}_c}{\rho_c} \Delta P \tag{9}$$

The performance index, which indicates the net enhancement or diminution of thermal performance relative to the pumping power, of the nanocoolant in comparison with the base fluid is calculated using Eq. (10).

$$\text{Performance Index} = \frac{U_{nc}/U_{bf}}{\Delta P_{nc}/\Delta P_{bf}} \tag{10}$$

5. UNCERTAINTY ANALYSIS

The RTDs and thermocouples used for measuring the temperature of coolants and air are associated with an uncertainty of 0.15°C and 0.25°C, respectively, with a 99.7% confidence level. The mass flow rate of radiator coolant is measured using a Coriolis mass flow meter (Make: Emerson - CMF025) with an accuracy of 0.2%, and a portable density meter (Make: Anton Paar, DMA 35) is used to measure the density of coolants with an uncertainty of $\pm$ 0.001 g/cm^3. The methodology adopted from the book by Venkateshan (2015) has been used to calculate the total uncertainty in overall as well as average heat transfer coefficients and pumping power. If R is a function of several variables,

$$R = f(x_1 x_2 x_3 x_4 \dots x_n) \tag{11}$$

then

$$\sigma_R = \sqrt{\sum_{i=1}^{n} \left(\frac{\partial R}{\partial x_i} * \sigma_{x_i} \right)^2} \tag{12}$$

Overall and average heat transfer coefficients are calculated with a maximum uncertainty of 8% and 6%, respectively. The measurement of pressure drop and pumping power is associated with $\pm$ 0.01 kPa and 3%, respectively.

6. VALIDATION OF EXPERIMENTAL SETUP

Before conducting experimentations in radiators, the same test rig is used to perform forced convective heat transfer studies with a circular stainless-steel tube as a test section with a 4 mm inside diameter, D, and an 850 mm length. The experiments are conducted with deionized water and alumina nanofluid (0.6 and 1 vol%) at a Reynolds number of 1600. The tube wall is heated by the joule heating method using a direct current transformer, and the local variation of heat transfer coefficient, h, along the nondimensional streamwise direction, x/D, is calculated for both the nanofluid and base fluid. The comparison of results with literature (Wen and Ding, 2004) as plotted in Fig. 4 shows good agreement with a maximum disparity of 10%, which is within the collective uncertainty limit of both experimental studies. The experimentations of alumina nanofluids in stainless steel tubes are conducted only for validation and comparison purposes, and the remaining experiments are performed with a radiator.

7. RESULTS AND DISCUSSION

Graphite nanocoolant and W/EG base fluid were used as coolants in the radiator. The coolant and air mass flow rates have varied throughout the experiments. The range of mass flow rates and the Reynolds number of coolants in the radiator tubes are presented in Table 2. The coolant mass flow rate used in the current work comprises the flow ranges studied by Oliet et al. (2007) and Selvam et al. (2017), as these articles report the pumping power or pressure drop across the radiator.

7.1 Overall Heat Transfer Coefficient based on Coolant Mass Flow Rate

Figure 5(a) shows the variation of the product of overall heat transfer coefficient and surface area (UA) of graphite nanocoolant and W/EG base fluid with respect to the coolant mass flow rate at two different air mass flow rates. Since the experiments are conducted on a particular radiator,

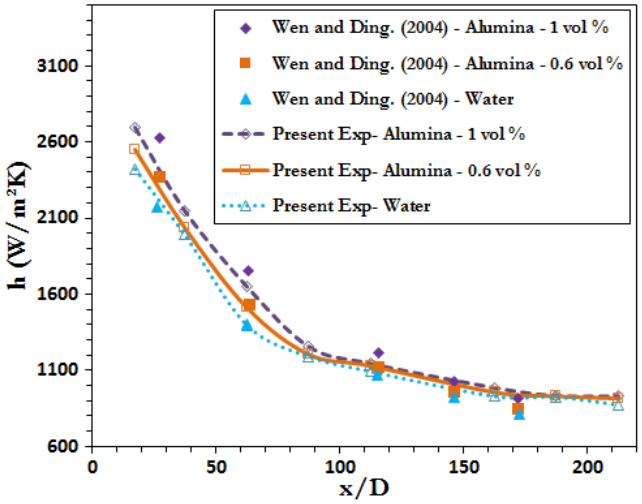

FIG. 4: Comparison of present study with Wen and Ding (2004) illustrates the axial variation of local heat transfer coefficient for alumina nanofluid and water base fluid at a Reynolds number of 1600

TABLE 2: Experimental parameters

Coolant mass flow rate	360–840 kg/h
Reynolds number	150–430
Air mass flow rate	300–1500 kg/h

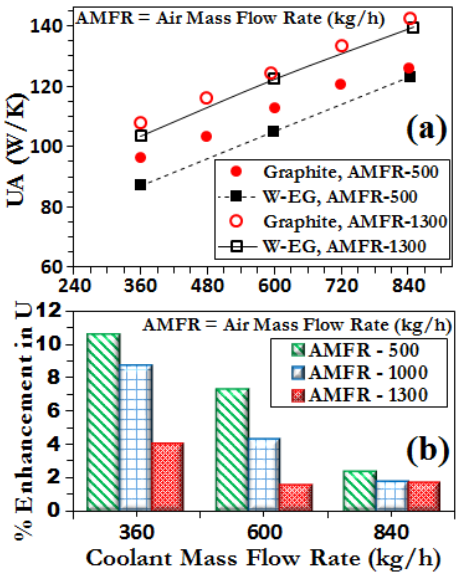

FIG. 5: Product of overall heat transfer coefficient and area (UA) for various coolant and air mass flow rates: (a) absolute value; (b) percentage enhancement

the surface area remains constant throughout all experiments and therefore, the graph of UA represents the behavior of overall heat transfer (U) itself. The coolant and air mass flow rates are varied over a range of 360 to 840 and 500 to 1300 kg/h, respectively, while conducting the present study. As the coolant mass flow rate increases, a linear increase in the overall heat transfer coefficient of the radiator can be observed. A similar rise in the overall heat transfer is observed with the increase of air mass flow rate also. The results show that the heat transfer performance of the graphite nanocoolant is higher than the base fluid in the entire range of experiments, whereas the enhancement in overall heat transfer coefficient reduces at higher air mass flow rate cases. This is because of harmonic dependency of the overall heat transfer coefficient on both the coolant side and air side heat transfer coefficients. As the air mass flow rate increases, the air side heat transfer coefficient increases and hence, its effect on the value of overall heat transfer coefficient also increases. Consequently, the significance of coolant side heat transfer on the overall heat transfer coefficient diminishes at higher air flow rate cases. The results indicate that the application of nanocoolants instead of conventional coolants can find adequate advantages in situations where the radiator air flow rate is insufficient, such as when the vehicle is stationary, idling, and so forth.

Figure 5(b) shows the percentage enhancement in the overall heat transfer coefficient of the graphite nanocoolant relative to the base fluid for different coolant mass flow rates (360, 600, and 840 kg/h) at three air mass flow rates (1300, 1000, 500 kg/h). An augmentation of 10.6% at a coolant mass flow rate of 360 kg/h can be observed at a lower air mass flow rate of 500 kg/h, and with an increase in the coolant mass flow rate to 840 kg/h the enhancement decreases to 2.4%. Also, while the air mass flow rate rises from 500 to 1300 kg/h, the enhancement of the coolant mass flow rate of 360 kg/h decreases from 10.6% to 4%. The results show that the graphite nanocoolant effectively enhances the overall heat transfer performance in the lower air mass flow rate experimental cases, whereas at higher air flow rate cases, the enhancement decreases because the overall performance is regardless of the coolant side heat transfer.

7.1.1 Average Heat Transfer Coefficient based on Reynolds Number

The graph shown in Fig. 6 represents the variation of the average heat transfer coefficient in the radiator while using a graphite nanocoolant or W/EG base fluid as the coolant with respect to the Reynolds number in a single radiator tube at two different air mass flow rates. The Reynolds number of W/EG base fluid is higher than graphite nanocoolant for the same mass flow rate due to the lower viscosity [Fig. 1(b)] and almost the same density of the base fluid when compared to the nanocoolant. The graphite nanocoolant exhibits higher thermal performance at the same Reynolds number, and the average heat transfer coefficient increases linearly with the increase in Reynolds number for all coolants.

7.1.2 Pressure Drop and Friction Factor

The pressure drop and friction factor across the radiator for graphite nanocoolant and W/EG base fluid at different Reynolds numbers are represented in Fig. 7. The relative difference in pressure drop between graphite nanocoolant and base fluid is negligibly small at lower Reynolds numbers, and as the Reynolds number increases, the difference become considerably large. This increase in relative change of pressure drop is due to the increase in particle drag at a higher Reynolds number. The pressure drop is observed to be increasing with air mass flow rate also. This is due to the temperature-dependent viscosity of the nanocoolant. At higher air mass flow

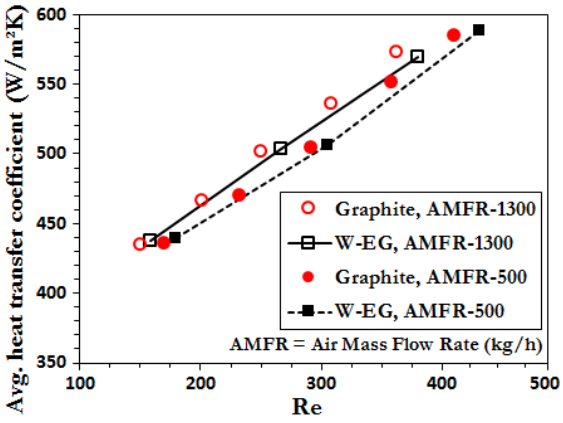

FIG. 6: Average heat transfer coefficient at various Reynolds numbers for both coolants at different air mass flow rates of 500 and 1300 kg/h

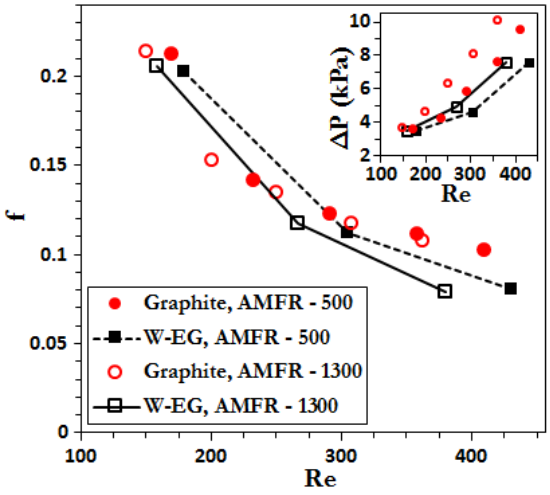

FIG. 7: Pressure drop and friction factor for various Reynolds numbers at air mass flow rates of 500 and 1300 kg/h

rates, the temperature of the nanocoolant decreases more, causing a proportional increase in the viscosity, which upsurges the pressure drop inside the radiator.

The friction factor of nanocoolant and base fluid is almost similar at lower Reynolds numbers, and as the Reynolds number increases the friction factor of nanocoolant intensifies a little more than the base fluid. The influence of air mass flow rate on the calculated friction factor values is marginally small.

7.2 Estimation of Overall Heat Transfer Coefficient based on Reynolds Number

Figure 8(a) shows the variation in the overall heat transfer coefficient of graphite nanocoolant and W/EG base fluid with respect to various coolant Reynolds numbers at two different air mass

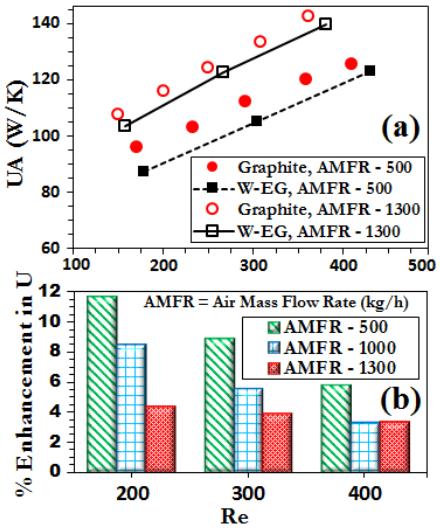

FIG. 8: Product of overall heat transfer coefficient and area (UA) for various Reynolds numbers at different air mass flow rates: (a) absolute value; (b) percentage enhancement

flow rates. In the case of both coolants, the overall heat transfer coefficient is observed to linearly increase with an increase in Reynolds number, and at a specific Reynolds number, it is directly dependent on the air mass flow rate. Graphite nanocoolant shows higher overall heat transfer coefficient than the base fluid in all experimental cases, and at a high air flow rate (1300 kg/h) the relative change in heat transfer is lower than that at a low air flow rate (500 kg/h).

The percentage enhancement in the overall heat transfer coefficient of graphite nanocoolant compared to the base fluid at different coolant Reynolds numbers and air mass flow rates is plotted in Fig. 8(b). Owing to the higher viscosity of nanocoolant, at a given mass flow rate the Reynolds number of nanocoolant is lower than the base fluid. Hence the data curves in Fig. 8(a) are fitted with a second-order polynomial to attain the value of overall heat transfer coefficient at a specific Reynolds number. A maximum enhancement of 11.7% at a Reynolds number of 200 can be observed at a lower air mass flow rate of 500 kg/h, and when the Reynolds number increases to 400 the enhancement decreases to 5.8%. As the air mass flow rate rises from 500 to 1300 kg/h, the heat transfer enhancement at a Reynolds number of 200 decreases from 11.7% to 4.3%.

7.3 Overall Heat Transfer Coefficient based on the Same Pumping Power Criteria

Variation in the UA of graphite nanocoolant and W/EG base fluid with respect to pumping power at different air mass flow rates is shown in Fig. 9(a). Because of the relatively lower viscosity of W/EG base fluid, it experiences lower pressure drop and hence lower pumping power across the radiator than the graphite nanocoolant at the same mass flow rate. The base fluid needs a maximum pumping power equal to 1.7 W at $\dot{m}_c = 840$ kg/h, whereas for graphite nanocoolant, the pumping power is 2.2 W. At a pumping power less than 1.7 W and 0.6 W, nanocoolant is showing higher heat transfer performance over the base fluid for an air mass flow rate of 500 kg/h and 1300 kg/h, respectively. Figure 9(b) illustrates the percentage variation in the overall heat

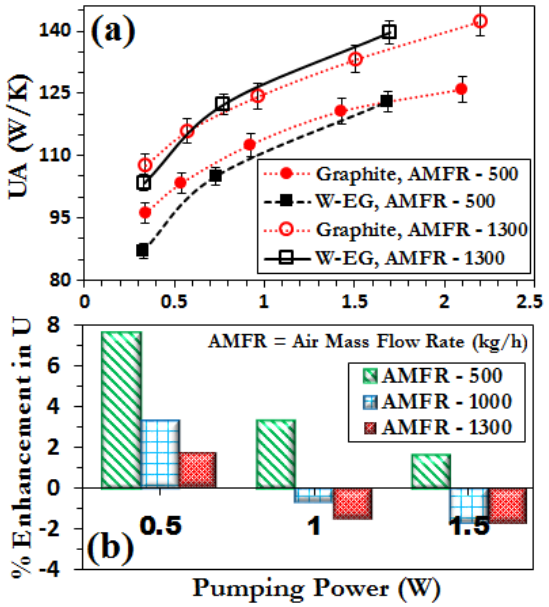

FIG. 9: Product of overall heat transfer coefficient and area (UA) for various pumping powers at different air mass flow rates: (a) absolute value; (b) percentage enhancement

transfer coefficient of graphite nanocoolant with respect to the base fluid for different pumping powers at three different air mass flow rates (500, 1000, 1300 kg/h). The comparison has been done for the range of pumping power (0.5–1.5 W) available for W/EG base fluid. The maximum enhancement of 7.6%, 3.2%, and 1.8%, respectively, for 500, 1000, and 1300 kg/h air flow rate cases is obtained at a lower pumping power (0.5 W), and as the pumping power rises the enhancement declines proportionately and is worsened to inferior values of 1.7%, –1.6%, and –1.7% at 1.5 W.

7.4 Estimation of Performance Index

The comparative results based on different criteria leads to contradictory conclusions. For example, the analysis based on the same Reynolds number criteria reveals that nanofluids show better performance for all cases than base fluid [Fig. 8(b)], whereas the same pumping power criteria shows that at a high pumping power range the performance of the nanocoolant is inferior to W/EG base fluid. Therefore, both criteria need to be simultaneously evaluated before considering graphite nanocoolant as a working fluid in radiators.

The performance index, which is the ratio of relative heat transfer enhancement to the relative pumping power, is plotted for a range of coolant mass flow rate at different air mass flow rates in Fig. 10. The values indicate that at lower coolant mass flow rates graphite nanocoolant performs better than the base fluid, but when the coolant mass flow rate increases, W/EG base fluid outperforms the nanocoolant. When the coolant mass flow rate increases from 300 kg/h to 840 kg/h, the performance index decreases from 1.08 to 0.82 at a constant air mass flow rate of 500 kg/h. This shows that at higher coolant flow rates, the addition of nanoparticles in the base

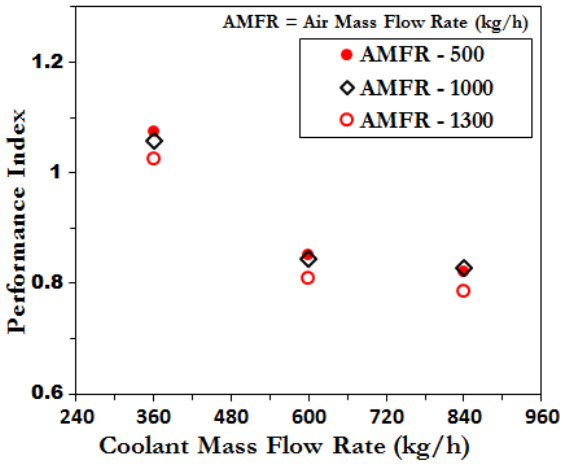

FIG. 10: Performance index of graphite nanocoolant compared to base fluid at various coolant and air mass flow rates

fluid causes a comparatively higher increase in pumping power than heat transfer rate. The performance index reduces from 1.08 to 1.03 with a variation of air mass flow rate from 500 kg/h to 1300 kg/h at a constant coolant flow rate of 360 kg/h.

8. CONCLUSIONS

Experimental evaluation of thermohydraulic performance of W/EG-based graphite nanocoolant (0.1 wt%) in an industrial vehicle radiator is conducted by utilizing an in-house test rig. Various measurements are completed to observe and analyze the morphology, stability, and thermophysical properties of the prepared graphite nanocoolant. The thermal performance is compared with the W/EG (50:50) base fluid on the basis of coolant mass flow rate, Reynolds number, and pumping power. Vital conclusions can be summarized as follows:

- The enhanced thermal conductivity of graphite nanoparticles relative to conventional heat transfer fluid (W/EG) enhances the single-phase overall heat transfer coefficient in radiators even with small concentrations (0.1 wt%) of graphite nanocoolant. The enhancement is higher at lower coolant flow rates and it weakens at higher flow rates because of the weaker dependence on the particle heat transport mechanisms. Maximum 10.6% overall heat transfer coefficient augmentation is experimentally observed at lower coolant and air mass flow rates of 360 kg/h and 500 kg/h, respectively. With an increase in the coolant mass flow rate to 840 kg/h the enhancement decreases to 2.4%, and as the air mass flow rates increases to 1300 kg/h, the enhancement decreases to 4%.
- The Reynolds number of W/EG base fluid is higher over graphite nanocoolant for the same mass flow rate because of the lower viscosity of the base fluid. Graphite nanocoolant shows a higher overall heat transfer coefficient than the base fluid, and a maximum enhancement of 11.7% is observed at lower Reynolds numbers and lower air mass flow rates. As the Reynolds number and air flow rate increases, the enhancement decreases similar to coolant mass flow rate cases.

- The pressure drop and friction factor are higher for nanocoolants and at higher Reynolds numbers the relative change in pressure drop increases due to the increase in particle drag force.
- At a pumping power less than 1.7 W and 0.6 W, the nanocoolant is showing higher heat transfer performance than base fluid for air mass flow rates of 500 kg/h and 1300 kg/h, respectively. The maximum enhancement of 7.6%, 3.2%, and 1.8%, respectively, for 500, 1000, and 1300 kg/h air flow rate cases have been obtained at lower pumping power (0.5 W), and as the pumping power rises the augmentation declines gradually and deteriorates to the lowest values of 1.7%, –1.6%, and –1.7% at 1.5 W.
- The performance index values indicate that, at lower coolant and air mass flow rates, graphite nanocoolant performs better than the base fluid, but when the flow rates increase the nanocoolant shows a reduction in overall performance. Hence the application of graphite nanocoolant may increase the pumping power in such cases where radiator flow rates are high, which can affect the vehicle performance unfavorably.

ACKNOWLEDGMENTS

This study is sponsored by the Defence Research and Development Organization (DRDO), India under the Grant No. ERIP/ER/RIC/2013/M/01/2194/D (R&D). The authors show gratitude toward various departments such as the Center Electronics Center (CEC); Department of Electrical Engineering for thermocouple/RTD calibration; Professor S. Ramprabhu, Department of Physics; Professor K.S. Reddy, Department of Mechanical Engineering; and the Department of Metallurgical and Materials Engineering of IIT Madras for the material characterization.

REFERENCES

Ahuja, A.S., Augmentation of Heat Transport in Laminar Flow of Polystyrene Suspensions. I. Experiments and Results, *J. Appl. Phys.*, vol. **46**, no. 8, pp. 3408–3416, 1975.

Akhavan-Zanjani, H., Saffar-Avval, M., Mansourkiaei, M., Sharif, F., and Ahadi, M., Experimental Investigation of Laminar Forced Convective Heat Transfer of Graphene–Water Nanofluid inside a Circular Tube, *Int. J. Thermal Sci.*, vol. **100**, pp. 316–323, 2016.

Azmi, W.H., Hamid, K.A., Mamat, R., Sharma, K.V., and Mohamad, M.S., Effects of Working Temperature on Thermo-Physical Properties and Forced Convection Heat Transfer of TiO_2 Nanofluids in Water–Ethylene Glycol Mixture, *Appl. Thermal Eng.*, vol. **106**, pp. 1190–1199, 2016.

Bergles, A.E. and Manglik, R.M., Current Progress and New Developments in Enhanced Heat and Mass Transfer, *J. Enhanced Heat Transf.*, vol. **20**, no. 1, 2013.

Berg, J.M., Romoser, A., Banerjee, N., Zebda, R., and Sayes, C.M., The Relationship between pH and Zeta Potential of $\sim$ 30 Nm Metal Oxide Nanoparticle Suspensions Relevant to in Vitro Toxicological Evaluations, *Nanotoxicology*, vol. **3**, no. 4, pp. 276–283, 2009.

Bianco, V., Marchitto, A., Scarpa, F., and Tagliafico, L.A., Computational Fluid Dynamics Modeling of Developing Forced Laminar Convection Flow of Al_2O_3–Water Nanofluid in a Two-Dimensional Rectangular Section Channel, *J. Enhanced Heat Transf.*, vol. **25**, nos. 4-5, 2018.

Choi, S.U. and Eastman, J.A., Enhancing Thermal Conductivity of Fluids with Nanoparticles, Argonne National Lab., IL, Rep. ANL/MSD/CP–84938; CONF-951135–29, 1995.

Chougule, S.S. and Sahu, S.K., Thermal Performance of Automobile Radiator Using Carbon Nanotube-Water Nanofluid—Experimental Study, *J. Thermal Sci. Eng. Appl.*, vol. **6**, no. 4, p. 041009, 2014.

Das, S.K., Putra, N., Thiesen, P., and Roetzel, W., Temperature Dependence of Thermal Conductivity Enhancement for Nanofluids, *J. Heat Transf.*, vol. **125**, no. 4, pp. 567–574, 2003.

Eastman, J.A., Choi, S.U.S., Li, S., Yu, W., and Thompson, L.J., Anomalously Increased Effective Thermal Conductivities of Ethylene Glycol-Based Nanofluids Containing Copper Nanoparticles, *Appl. Phys. Lett.*, vol. **78**, no. 6, pp. 718–720, 2001.

Heris, S.Z., Esfahany, M.N., and Etemad, G., Investigation of CuO/Water Nanofluid Laminar Convective Heat Transfer through a Circular Tube, *J. Enhanced Heat Transf.*, vol. **13**, no. 4, 2006.

Huang, J., Wang, X., Long, Q., Wen, X., Zhou, Y., and Li, L., Influence of pH on the Stability Characteristics of Nanofluids, in *Proc. IEEE: Int. Symposium on Photonics and Optoelectronics (SOPO)*, Wuhan, China, pp. 1–4, 2009.

Hussein, A.M., Bakar, R.A., and Kadirgama, K., Study of Forced Convection Nanofluid Heat Transfer in the Automotive Cooling System, *Case Studies Thermal Eng.*, vol. **2**, pp. 50–61, 2014.

Lee, J.H., Hwang, K.S., Jang, S.P., Lee, B.H., Kim, J.H., Choi, S.U., and Choi, C.J., Effective Viscosities and Thermal Conductivities of Aqueous Nanofluids Containing Low Volume Concentrations of Al_2O_3 Nanoparticles, *Int. J. Heat Mass Transf.*, vol. **51**, nos. 11-12, pp. 2651–2656, 2008.

Leong, K.Y., Saidur, R., Kazi, S.N., and Mamun, A.H., Performance Investigation of an Automotive Car Radiator Operated with Nanofluid-Based Coolants (Nanofluid as a Coolant in a Radiator), *Appl. Thermal Eng.*, vol. **30**, no. 17, pp. 2685–2692, 2010.

Liao, L., Liu, Z., and Bao, R., Forced Convective Flow Drag and Heat Transfer Characteristics of CuO Nanoparticle Suspensions and Nanofluids in a Small Tube, *J. Enhanced Heat Transf.*, vol. **17**, no. 1, 2010.

Li, Q., Xuan, Y., and Wang, J., Investigation on Convective Heat Transfer and Flow Features of Nanofluids, *J. Heat Transf.*, vol. **125**, no. 1, pp. 151–155, 2003.

Liu, K.V., Choi, U.S., and Kasza, K.E., Measurements of Pressure Drop and Heat Transfer in Turbulent Pipe Flows of Particulate Slurries, Argonne National Lab., IL, Rep. ANL-88-15,1988.

Lv, J., Zhou, L., Bai, M., Liu, J.W., and Xu, Z., Numerical Simulation of the Improvement to the Heat Transfer within the Internal Combustion Engine by the Application of Nanofluids, *J. Enhanced Heat Transf.*, vol. **17**, no. 1, 2010.

Meyer, J.P., Adio, S.A., Sharifpur, M., and Nwosu, P.N., The Viscosity of Nanofluids: A Review of the Theoretical, Empirical, and Numerical Models, *Heat Transf. Eng.*, vol. **37**, no. 5, pp. 387–421, 2016.

M'hamed, B., Sidik, N.A.C., Akhbar, M.F.A., Mamat, R., and Najafi, G., Experimental Study on Thermal Performance of MWCNT Nanocoolant in Peroduakelisa 1000cc Radiator System, *Int. Commun. Heat Mass Transf.*, vol. **76**, pp. 156–161, 2016.

Nieh, H.M., Teng, T.P., and Yu, C.C., Enhanced Heat Dissipation of a Radiator Using Oxide Nano-Coolant, *Int. J. Thermal Sci.*, vol. **77**, pp. 252–261, 2014.

Oliet, C., Oliva, A., Castro, J., and Pérez-Segarra, C.D., Parametric Studies on Automotive Radiators, *Appl. Thermal Eng.*, vol. **27**, nos. 11-12, pp. 2033–2043, 2007.

Pak, B.C. and Cho, Y.I., Hydrodynamic and Heat Transfer Study of Dispersed Fluids with Submicron Metallic Oxide Particles, *Exper. Heat Transf. Int. J.*, vol. **11**, no. 2, pp. 151–170, 1998.

Peyghambarzadeh, S.M., Hashemabadi, S.H., Jamnani, M.S., and Hoseini, S.M., Improving the Cooling Performance of Automobile Radiator with Al_2O_3/Water Nanofluid, *Appl. Thermal Eng.*, vol. **31**, no. 10, pp. 1833–1838, 2011.

Peyghambarzadeh, S.M., Hashemabadi, S.H., Naraki, M., and Vermahmoudi, Y., Experimental Study of Overall Heat Transfer Coefficient in the Application of Dilute Nanofluids in the Car Radiator, *Appl. Thermal Eng.*, vol. **52**, no.1, pp. 8–16, 2013.

Sandhu, H., Gangacharyulu, D., and Singh, M.K., Experimental Investigations on the Cooling Performance of Microchannels Using Alumina Nanofluids with Different Base Fluids, *J. Enhanced Heat Transf.*, vol.

25, no. 3, 2018.

Selvam, C., Lal, D.M., and Harish, S., Enhanced Heat Transfer Performance of an Automobile Radiator with Graphene-Based Suspensions, *Appl. Thermal Eng.*, vol. **123**, pp. 50–60, 2017.

Shah, R.K. and Sekulic, D.P., *Fundamentals of Heat Exchanger Design*, Hoboken, NJ: John Wiley & Sons, Inc., 2003.

Suganthi, K.S. and Rajan, K.S., Temperature-Induced Changes in ZnO–Water Nanofluid: Zeta Potential, Size Distribution and Viscosity Profiles, *Int. J. Heat Mass Transf.*, vol. **55**, nos. 25-26, pp. 7969–7980, 2012.

Teng, T.P. and Yu, C.C., Heat Dissipation Performance of MWCNTs Nano-Coolant for Vehicle, *Exper. Thermal Fluid Sci.*, vol. **49**, pp. 22–30, 2013.

Utomo, A.T., Haghighi, E.B., Zavareh, A.I., Ghanbarpourgeravi, M., Poth, H., Khodabandeh, R., Palm, B., and Pacek, A.W., The Effect of Nanoparticles on Laminar Heat Transfer in a Horizontal Tube, *Int. J. Heat Mass Transf.*, vol. **69**, pp. 77–91, 2014.

Vajjha, R.S., Das, D.K., and Kulkarni, D.P., Development of New Correlations for Convective Heat Transfer and Friction Factor in Turbulent Regime for Nanofluids, *Int. J. Heat Mass Transf.*, vol. **53**, no. 21, pp. 4607–4618, 2010.

Venkateshan, S.P., *Mechanical Measurements*, 2nd ed., West Sussex, UK: John Wiley & Sons Ltd., 2015.

Walvekar, R., Siddiqui, M.K., Ong, S., and Ismail, A.F., Application of CNT Nanofluids in a Turbulent Flow Heat Exchanger, *J. Exper. Nanosci.*, vol. **11**, no. 1, pp. 1–17, 2016.

Wen, D. and Ding, Y., Experimental Investigation into Convective Heat Transfer of Nanofluids at the Entrance Region under Laminar Flow Conditions, *Int. J. Heat Mass Transf.*, vol. **47**, no. 24, pp. 5181–5188, 2004.

Xuan, Y. and Li, Q., Heat Transfer Enhancement of Nanofluids, *Int. J. Heat Fluid Flow*, vol. **21**, no. 1, pp. 58–64, 2000.

Yang, Y., Zhang, Z.G., Grulke, E.A., Anderson, W.B., and Wu, G., Heat Transfer Properties of Nanoparticle-in-Fluid Dispersions (Nanofluids) in Laminar Flow, *Int. J. Heat Mass Transf.*, vol. **48**, no. 6, pp. 1107–1116, 2005.

Zuccaro, L., Krieg, J., Desideri, A., Kern, K., and Balasubramanian, K., Tuning the Isoelectric Point of Graphene by Electrochemical Functionalization, *Sci. Rep.*, vol. **5**, p. 11794, 2015.